ARTICLE

Osteopontin protects against lung injury caused by extracellular histones

Gopinath Kasetty[1], Praveen Papareddy[2], Ravi K. V. Bhongir[1], Mohamad N. Ali[1], Michiko Mori[3], Malgorzata Wygrecka[4], Jonas S. Erjefält[3], Anna Hultgårdh-Nilsson[3], Lena Palmberg[5], Heiko Herwald[2] and Arne Egesten[1]

Extracellular histones are present in the airways because of cell death occurring during inflammation. They promote inflammation and cause tissue damage due to their cationic nature. The anionic phosphoglycoprotein osteopontin (OPN) is expressed at high levels during airway inflammation and has been ascribed both pro- and anti-inflammatory roles. In this study, it was hypothesized that OPN may neutralize the harmful activities of extracellular histones at the airway mucosal surface. In a model of histone-induced acute lung injury, OPN$^{-/-}$ mice showed increased inflammation and tissue injury, and succumbed within 24 h, whereas wild-type mice showed lower degrees of inflammation and no mortality. In lipopolysaccharide-induced acute lung injury, wild-type mice showed less inflammation and tissue injury than OPN$^{-/-}$ mice. In bronchoalveolar lavage fluid from ARDS patients, high levels of OPN and also histone–OPN complexes were detected. In addition, OPN bound to histones with high affinity in vitro, resulting in less cytotoxicity and reduced formation of tissue-damaging neutrophil extracellular traps (NETs). The interaction between OPN and histones was dependent on posttranslational modification of OPN, i.e., phosphorylation. The findings demonstrate a novel role for OPN, modulating the pro-inflammatory and cytotoxic properties of free histones.

INTRODUCTION

Acute respiratory distress syndrome (ARDS) is a severe clinical condition characterized by acute onset, opacities on chest radiographs, presence of proteinaceous edema, severe hypoxemia, and impaired carbon dioxide exchange.[1,2] Etiologically, ARDS can result from both pulmonary and extra-pulmonary causes, including sepsis, severe pulmonary infection, and trauma.[3] ARDS is preceded by acute lung injury (ALI), the latter caused by an exaggerated and prolonged inflammatory response. Inflammation and tissue injury result in cell death, including necrosis, apoptosis, and release of neutrophil extracellular traps (NETs).[4] This cell death results in release of intracellular molecules, i.e., danger-associated molecular patterns (DAMPs), further promoting inflammation and cell death, aggravating the condition. An important class of DAMPs is the highly cationic extracellular histones, executing both pro-inflammatory and cytotoxic effects.[4–6] Other examples of factors that trigger ALI are pathogen-associated molecular patterns (PAMPs), for example, lipopolysaccharides (LPS) released by Gram-negative bacteria, resulting in dysregulated inflammation and ALI.[7,8] The accumulation of neutrophils in ALI leads to the formation of NETs and sustained release of extracellular histones, aggravating tissue and organ dysfunction.[9–12] When present in the extracellular environment, the cationic histones have potent cytotoxic activities through membrane damage.[13–16] Extracellular histones also serve as alarmins and their pro-inflammatory effects are mediated though activation of TLR2, TLR4, and TLR9.[17–19]

Osteopontin (OPN) is a multifunctional phosphoglycoprotein belonging to a small family of proteins named SIBLINGs (small integrin-binding ligand, N-linked glycosylation) and is found in numerous tissues of the body, including bone, and is also secreted into body fluids by epithelial cells, for example, airway epithelial cells.[20] In addition, OPN is expressed by alveolar macrophages.[21] OPN is constitutively expressed in the airways during healthy conditions and high levels can be detected in sputum during states of disease characterized by prolonged airway inflammation, i.e., chronic obstructive pulmonary disease (COPD), cystic fibrosis (CF), and asthma.[22–24] It has been assigned several functions including promotion of Th1 inflammation, recruitment of neutrophils, and matrix remodeling.[25] Despite having some cytokine-like properties, OPN is larger (migrating at around 45–75 kD in SDS-PAGE) and present at higher concentrations than most cytokines, suggesting that it has several functions.[20] Some studies implicate harmful activities of OPN, for example, during systemic inflammation.[26] However, beneficial roles have been demonstrated in several models, including tissue protection during ischemia and reperfusion injury.[27–31] Osteopontin is a highly anionic molecule while many pro-inflammatory mediators are cationic. This includes many chemokines as well as DAMPs, promoting inflammation and tissue injury.[32,33] Several electrostatic interactions have been demonstrated, protecting host tissue from histone-induced damage.[34,35]

We set out to investigate whether OPN protects against the harmful effects of extracellular histones at the airway mucosal

---

[1]Respiratory Medicine & Allergology, Lund University and Skåne University Hospital, Lund, Sweden; [2]Infection Medicine, Department of Clinical Sciences, Lund University and Skåne University Hospital, Lund, Sweden; [3]Department of Experimental Medical Science, Lund University and Skåne University Hospital, Lund, Sweden; [4]Department of Biochemistry, German Center of Lung Research, University of Giessen, Giessen, Germany and [5]Work Environment Toxicology, Institute of Environmental Medicine, Karolinska Institutet, Solna, Sweden
Correspondence: Gopinath Kasetty (Gopinath.Kasetty@med.lu.se)

surface, not least because of the parallel increase of both in the conducting airways during severe inflammation. Here, we demonstrate a key role for OPN, protecting against lung tissue injury during airway inflammation.

RESULTS

Osteopontin protects mice from histone-induced acute lung injury
To investigate whether OPN has a protective effect against the pro-inflammatory and cytotoxic properties of extracellular histones in vivo, wild-type (WT) and OPN$^{-/-}$ mice were instilled with calf thymus histones (CTH; 50 μg/g body weight) intranasally to induce ALI. The survival of the mice was monitored for 7 days (Fig. 1a) (only the course during the first 72 h is shown in the figure). The OPN$^{-/-}$ mice succumbed within 24 h, whereas the WT mice survived the histone challenge. Interestingly, co-instillation of CTH with recombinant murine OPN (200 μg/mouse) rescued the OPN$^{-/-}$ mice ($n = 6$), indicating that OPN may bind to histones and neutralize their toxic effects (Fig. 1b). Circulating histones cause lung injury in trauma patients.[36] To investigate if a protective effect from OPN was achieved in a severe model of systemic inflammation, CTH were injected intravenously in the absence and presence of OPN. Preincubation of CTH with OPN rescued the mice while CTH alone was lethal within 1 h (Fig. 1c). The levels of OPN in BALF of WT mice were determined, and found to be significantly increased 16 h after histone-induced ALI (Fig. 1d). Plasma, BALF, and lungs were collected 16 h after histone challenge for evaluation of inflammatory mediators and lung damage. The levels of LDH and albumin, indicating lung injury, were measured in BALF samples. OPN$^{-/-}$ mice had significantly higher levels of both LDH and albumin after histone challenge than WT mice (Fig. 1e, f), indicating increased cytotoxicity and capillary leakage in these animals. Furthermore, the overall tissue damage in mice was assessed determining aspartate aminotransferase (AST) levels in plasma. Significant increases were observed in OPN$^{-/-}$ mice compared to WT mice (Fig. 1g). The increased degree of tissue damage in the lungs of OPN$^{-/-}$ mice was further confirmed by routine histology and scanning electron microscopy of lung sections, where increased lung damage was seen. This included hyaline membranes, proteinaceous debris filling the airspaces, alveolar septal thickening, infiltration of immune cells, and hemorrhage (Fig. 1h, i). The levels of selected cytokines, chemokines, and growth factors were measured in BALF to assess the degree of inflammation. As shown by the heat map representation, OPN$^{-/-}$ mice had significantly higher levels of inflammatory mediators than WT mice (Fig. 1i). In particular, important pro-inflammatory cytokines such as IL-6, IFN-α, KC, MCP-1, and TNF-α—and also the anti-inflammatory cytokine IL-10—were significantly increased in OPN$^{-/-}$ mice (Fig. 1j). Overall, these results suggest that OPN has important protective roles in neutralizing both the cytotoxic and the pro-inflammatory actions of histones in a murine model of ALI.

OPN protects against tissue damage and dampens inflammation in LPS-induced acute lung injury
To further study the biological relevance of OPN, modulating tissue injury and inflammation in a more physiological context, WT and OPN$^{-/-}$ mice were instilled intranasally with 2 μg/g body weight of E. coli LPS to induce ALI. All mice were killed 8 h after the LPS challenge. BALF and lung tissues were collected to determine the degree of lung damage, release of extracellular histones, and inflammatory mediators. Following LPS challenge, extracellular histones were detected in BALF using anti-H3 antibodies and western blot. A significant increase of extracellular histones was found in BALF of OPN$^{-/-}$ mice compared to WT mice (Fig. 2a). LPS instillation significantly increased the pulmonary OPN concentration in WT mice as measured using ELISA (Fig. 2b). To assess the severity of lung damage induced by LPS in WT and OPN$^{-/-}$ mice,

dry/wet weight ratios of lungs, LDH, and albumin levels in BALF were quantified (Fig. 2c, d, e). Consistent with the histone-induced ALI model, LPS challenge in OPN$^{-/-}$ mice caused increased edema and higher release of LDH and albumin, indicating increased tissue damage during inflammation. Hematoxylin and eosin staining and scanning electron microscopy of lung sections further confirmed the pronounced severity of ALI in OPN$^{-/-}$ mice after LPS challenge (Fig. 2f, g). In addition, the levels of inflammatory mediators also showed significantly higher levels of several pro-inflammatory cytokines, chemokines, and growth factors in the BALF of OPN$^{-/-}$ mice (Fig. 2h, i), further confirming the dampening effect of OPN during ALI. In BALF, the levels of inflammatory cells were slightly lower in OPN$^{-/-}$ mice but only significant in the case of lymphocytes (Supplementary Figure 1).

The significance of OPN was underlined using a model of *Pseudomonas aeruginosa* airway infection. In this model, WT animals show a prolonged survival compared to OPN$^{-/-}$ animals (Supplementary Figure 2a). The presence of significantly lower number of cfu in the BALF and lung tissue of WT mice correlated to their prolonged survival compared to OPN$^{-/-}$ mice (Supplementary Figure 2b). The levels of OPN in the BALF of WT mice were significantly increased post infection compared to mice treated with vehicle alone (Supplementary Figure 2c). The levels of the pro-inflammatory cytokine IL-6 were also significantly lower in the WT mice (Supplementary Figure 2d). Taken together, these findings suggest both protective and immunomodulatory functions of OPN.

Elevated levels of histone–OPN complexes in BALF of ARDS patients and individuals with lung injury
In ARDS patients, there is a substantial increase of extracellular histones present in the airways.[37] To investigate whether OPN is increased in ARDS and form complexes with extracellular histones, BALF from ARDS patients ($n = 22$) and healthy individuals ($n = 14$) were investigated. The clinical phenotypes of these individuals are described in Supplementary Table 1. The levels of OPN in the BALF of ARDS patients were significantly higher compared to healthy individuals (Fig. 3a). Furthermore, increased presence of histone–OPN complexes in the BALF samples of ARDS patients compared to healthy individuals was demonstrated (Fig. 3b).

Short-term exposure to swine dust can cause acute airway inflammation, including increases in the key pro-inflammatory cytokines IL-6 and IL-8.[38] We therefore used this model to investigate whether OPN expression is upregulated in human airways in parallel with markers of tissue damage (i.e., histones, LDH, and albumin). BALF was obtained from healthy volunteers before and 24 h after a 3-h exposure to swine dust on a swine farm. Extracellular histones were indeed detected in the BALF from some individuals who were exposed to swine dust (Fig. 3c). Significant increases in OPN levels in BALF were also observed in these subjects after exposure to swine dust (Fig. 3d). Similarly to ARDS patients, increased levels of histone–OPN complexes were detected in BALF after exposure to swine dust (Fig. 3e). In addition, the indicators of lung damage LDH and albumin[39] were significantly increased after exposure to swine dust (Fig. 3f). There was a parallel increase of albumin and OPN, which is similar to what was seen in the animal model with histone-induced ALI.

In COPD and CF, increased levels of both NETs and extracellular histones have been described.[40–42] In addition, these conditions are associated with increased levels of OPN in the airways.[22,23] Therefore, a possible co-localization between OPN and extracellular histones was investigated in lung tissues obtained from patients suffering from these states of disease (i.e., COPD and CF) using immunohistochemistry (characteristics of patients with CF, COPD, and controls are described in Supplementary Table 2). High presence of histones and OPN was detected in mucus plugs that also contained cells and cellular debris, and on the apical surface of bronchial epithelial cells (Fig. 3g). Co-localization of histones
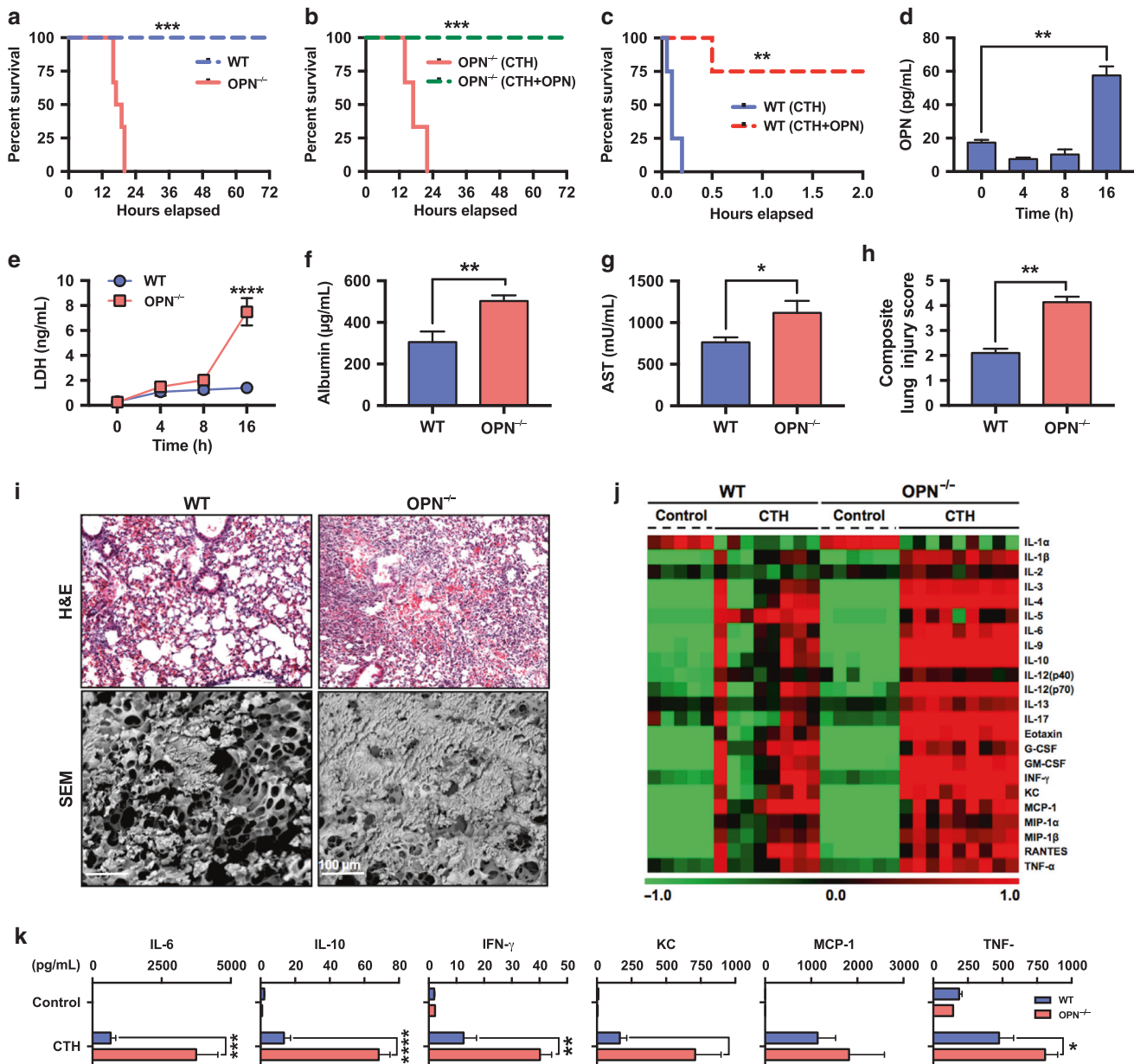
Osteopontin protects against lung injury caused by extracellular histones
G. Kasetty et al.

41

Fig. 1 Osteopontin prevents acute lung injury caused by extracellular histones. **a** Survival curves of wild-type (WT) and osteopontin (OPN)$^{-/-}$ mice after intranasal instillation of calf thymus histones (CTH; 50 µg/g of body weight). Survival was monitored for 7 days (only the course during the first 72 h is shown in the figure). $n = 6$ per group; ***$P = 0.0007$ between groups. **b** Survival curves of OPN$^{-/-}$ mice after intranasal instillation of CTH in buffer alone or together with recombinant mOPN. The survival was monitored for 7 days (only the course during the first 72 h is shown in the figure). $n = 8$ per group; ***$P = 0.0007$ between groups. **c** Survival curves of WT mice after intravenous injection of CTH (75 µg/g of body weight) in buffer alone or together with OPN (100 µg/mice). The survival was monitored for 24 h (only the course during the first 2 h is shown in the figure). $n = 4$ per group; **$P = 0.0069$ between groups. **d** The concentrations of OPN in the bronchoalveolar lavage fluid (BALF) of WT mice 0, 4, 8, and 16 h after instillation of CTH. $n = 6$ per group; *$P = 0.002$, ****$P < 0.0001$ between groups. **e, f** To assess lung injury, lactate dehydrogenase (LDH; reflecting cytotoxicity) and alveolar albumin (reflecting capillary leakage) levels were determined in BALF using ELISA after histone-induced lung injury in WT and OPN$^{-/-}$ mice, respectively. $n = 8$ per group; ****$P = < 0.0001$, **$P = 0.0022$ between groups. **g** The levels of AST in plasma were assessed in order to reflect the effects on overall organ damage following histone-induced lung injury. $n = 6$ per group; *$P = 0.035$ between groups. **h** A blinded evaluation of the tissue injury was performed on hematoxylin & eosin-stained slides using a lung injury scoring system, showing increased lung injury in OPN$^{-/-}$ mice. $n = 6$ per group; **$P = 0.0022$ between groups. **i** Representative hematoxylin & eosin staining and scanning electron microscopy images of lung sections, showing differences in lung damage when comparing WT and OPN$^{-/-}$ mice, as indicated on each panel. Scale bars = 100 µm. **j** Heat map representation of cytokine profiles in BALF of WT and OPN$^{-/-}$ mice after histone-induced lung injury. Inflammatory mediators were measured using multiplex bead assay 16 h after intranasal instillation of CTH. **k** Bar graph representation of selected key pro-inflammatory mediators. Data are mean ± SEM; $n = 9$ per histone-exposed group, $n = 5$ per control group

Osteopontin protects against lung injury caused by extracellular histones
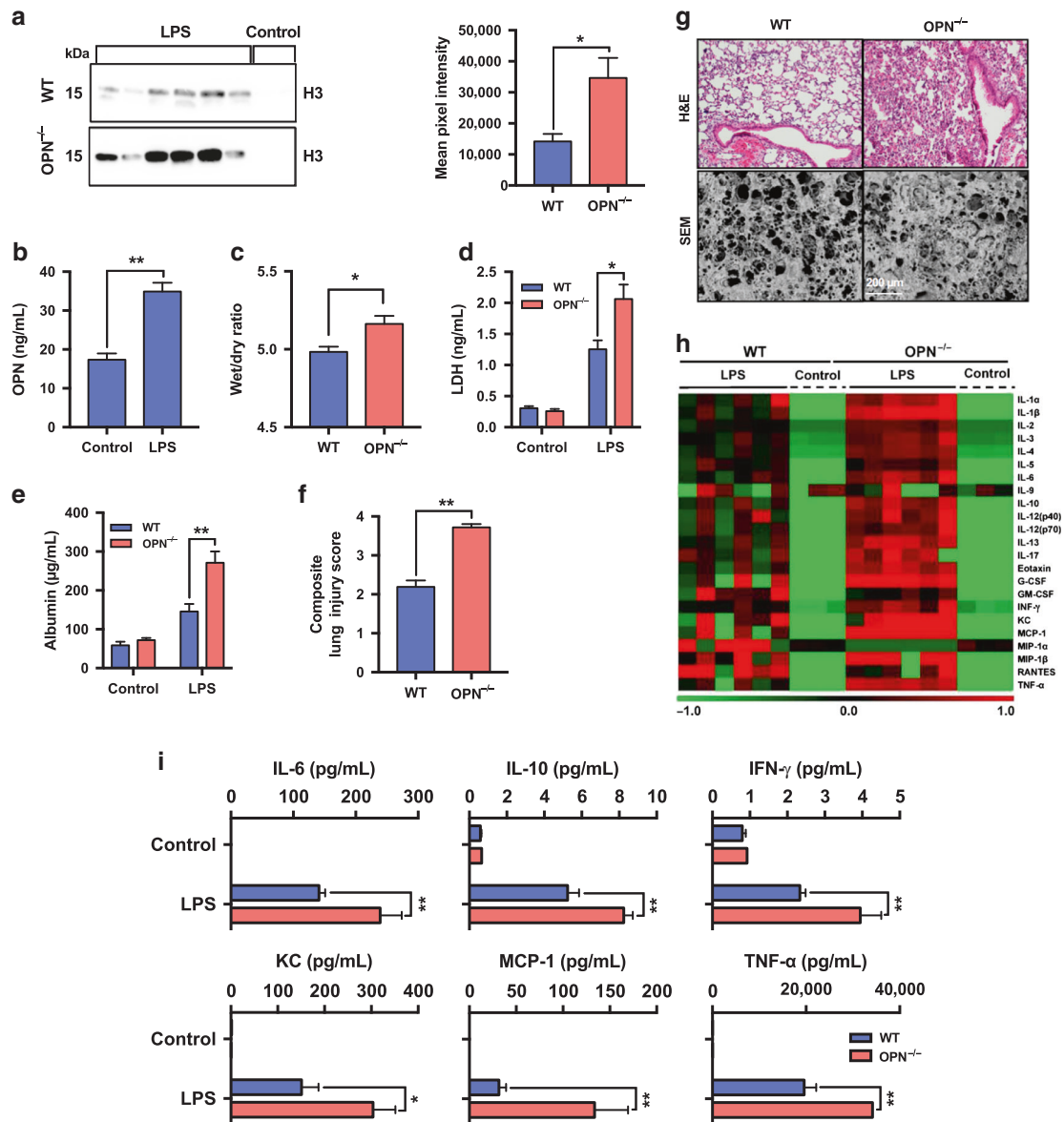G. Kasetty et al.

42

Fig. 2 Osteopontin dampens inflammation and tissue injury in LPS-induced acute lung injury. To induce airway inflammation, LPS (2 µg/g derived from *E. coli*) was instilled intranasally in WT and OPN$^{-/-}$ mice. The mice were killed 8 h after the LPS challenge, and BALF, lung tissue, and plasma were collected. **a** The levels of histone H3 in BALF of WT and OPN$^{-/-}$ mice after LPS exposure were examined using western blot analysis. The graphical representation of pixel intensity (right panel) indicated significant differences between WT and OPN$^{-/-}$ mice. $n = 6$ per group; $*P = 0.0411$ between groups. **b** The concentrations of OPN in the bronchoalveolar lavage fluid (BALF) of WT mice 8 h after instillation of LPS ($n = 6$ per group; $**P = 0.0043$ between groups). **c** The dry/wet ratios of lungs were determined to compare pulmonary edema in WT and OPN$^{-/-}$ mice. $n = 7$ in WT group and $n = 4$ in OPN$^{-/-}$ group; $*P = 0.0121$ between groups. **d, e** LDH and albumin levels in BALF of WT and OPN$^{-/-}$ mice were determined in order to assess lung damage. $n = 6$ per group; $*P = 0.0152$, $**P = 0.0082$ between groups. OPN$^{-/-}$ mice had higher levels of LDH and albumin, reflecting more damage to the lungs. **f** Blind evaluation of the tissue injury was performed on hematoxylin & eosin-stained slides using a lung injury scoring system, showing increased lung injury in OPN$^{-/-}$ mice. $n = 6$ per group; $**P = 0.0022$ between groups. **g** Representative hematoxylin & eosin and scanning electron microscopy images of lung sections of LPS-induced ALI, showing differences in lung damage between WT and OPN$^{-/-}$ mice. **h** Heat map representation of inflammatory mediators measured in the BALF of WT and OPN$^{-/-}$ mice after LPS challenge, using multiplex bead assay. **i** Bar graph of some selected key pro-inflammatory mediators. $n = 6$ per LPS group, $n = 3$ per control group

and OPN was apparent on the apical surface of bronchial epithelial cells.

OPN binds and inhibits the cytotoxic and hemolytic effects of histones
To determine the binding kinetics between OPN and histones, surface plasmon resonance (SPR) was performed. The individual histone subunits were immobilized on a sensor chip and OPN was then injected over the chip. The sensorgram curves showed

strong binding incidence with association and dissociation curves between H1, H2A, H2B, H3.1, H4, and OPN (Fig. 4a).

To investigate whether OPN protects against the cytotoxic effects of extracellular histones, we investigated release of LDH from human bronchial epithelial cells (BEAS-2B), membrane permeability effects using endothelial cells (EA.hy926), and hemolysis of human erythrocytes. After initial titration experiments, cells were incubated with either individual histones (H1, H2A, H2B, H3.1, and H4) or CTH alone, or histones preincubated
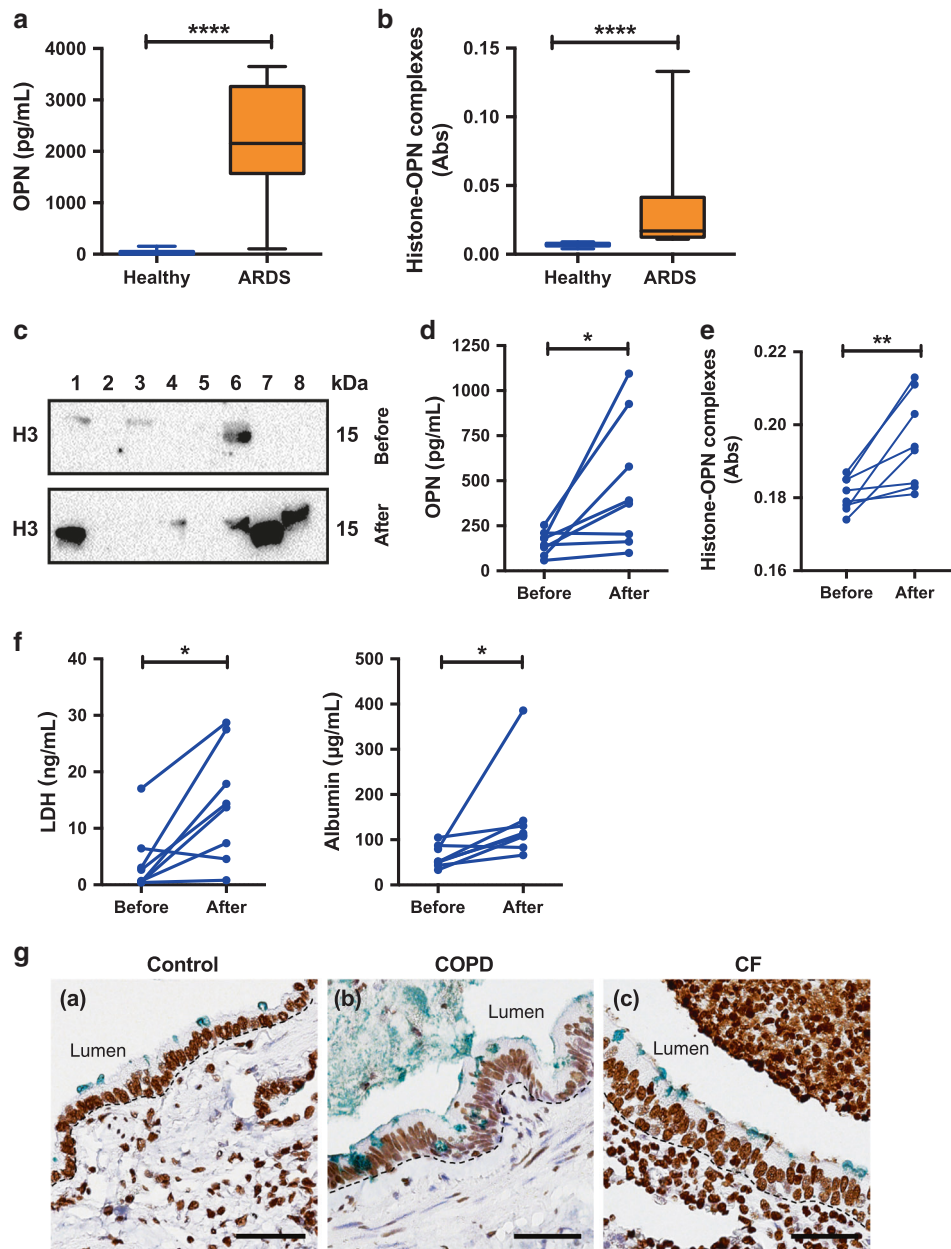
Osteopontin protects against lung injury caused by extracellular histones
G. Kasetty et al.

43

Fig. 3 Osteopontin binds to extracellular histones present in BALF of patients with acute respiratory distress syndrome (ARDS) and individuals with lung injury. **a** Levels of OPN in the BALF of ARDS patients ($n = 21$) and healthy control ($n = 14$) were assessed by ELISA. OPN levels were significantly elevated in ARDS patients. ****$P = < 0.001$. **b** Levels of histone–OPN complexes in BALF of ARDS patients ($n = 21$) and healthy control ($n = 12$) BALF. ****$P = < 0.001$. **c** Western blot analysis of BALF samples detected histone H3 after exposure of humans to swine dust. Healthy individuals (six men and two women) were exposed to swine dust for 3 h on a swine farm, and BALF was retrieved before and 24 h after the exposure. Four out of eight individuals had increased amounts of extracellular histones H3 in BALF after exposure to the swine dust. **d** The OPN levels in BALF were also elevated in individuals after exposure to swine dust. $n = 8$; *$P = 0.038$. **e** Levels of histone–OPN complexes in the BALF were significantly increased after exposure to swine dust. $n = 8$; **$P = 0.0188$. **f** The LDH levels in BALF were determined to assess lung damage, and were significantly higher after exposure to swine dust. Similarly, the levels of albumin were also significantly elevated, indicating increased pulmonary vascular permeability after exposure to swine dust. $n = 8$; *$P = 0.015$, **$P = 0.003$. **g** IHC showing OPN and histone (H4) co-localization in the small airways in lung sections from (a) healthy individuals, (b) COPD patients, and (c) CF patients. Histone H4 is visualized by a brown peroxidase reaction while OPN appears in green. Scale bar = 100 µm

with OPN at a ratio of 1:1. The individual histones H2A, H2B, and to some extent H4 caused release of LDH, indicating cytotoxic effects on epithelial cells, which was reduced after preincubation of the histones with OPN (Fig. 4b). Incubation with OPN alone did not induce cytotoxic effects in bronchial epithelial cells. CTH caused strong release of LDH from epithelial cells, which was considerably reduced after preincubation with OPN. Similarly, OPN preincubation with histones reduced the permeability across the endothelial

cell monolayer (Fig. 4c). In hemolysis experiments, in particular, histone H4 showed strong activity. In all cases, OPN showed a strong reducing effect on the hemolysis (Fig. 4d). Taken together, these results indicate that OPN has a strong protective effect against histone-induced cytotoxicity and hemolysis in vitro.

To address if OPN also binds to citrullinated histones, SPR was used to compare binding affinities of OPN to native and citrullinated histone tails derived from H2A, H3, and H4
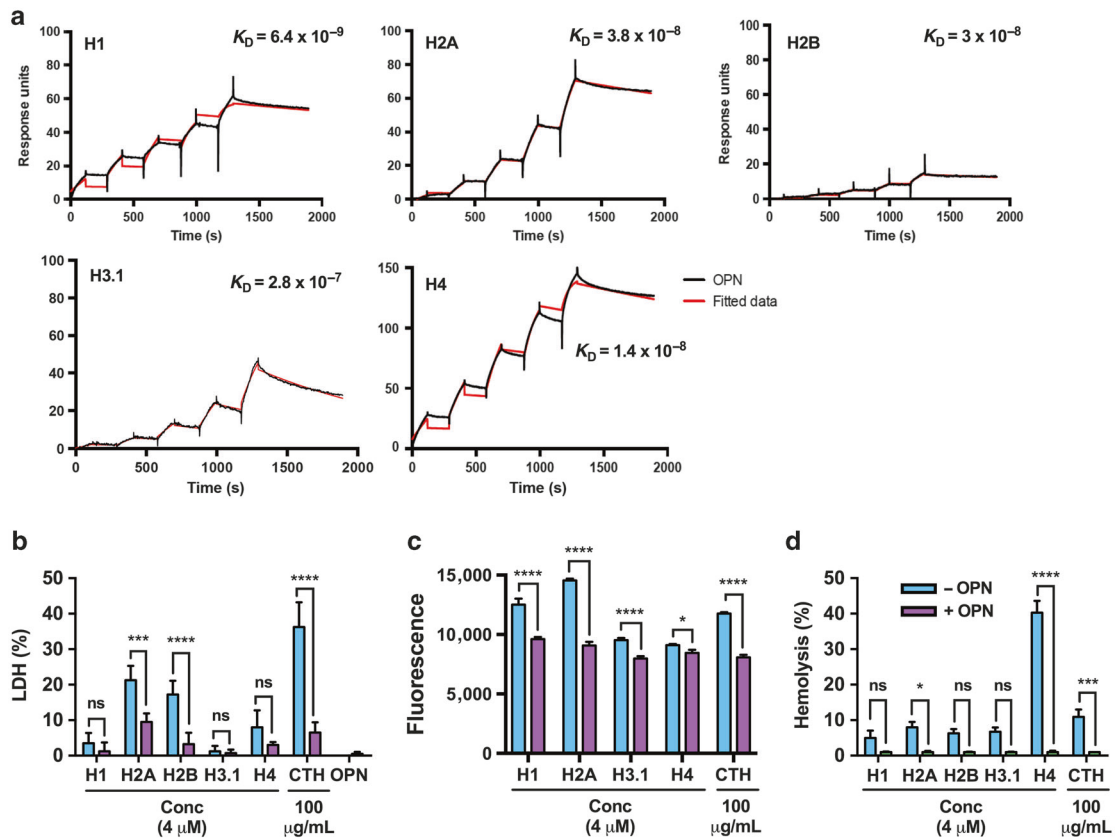
Osteopontin protects against lung injury caused by extracellular histones
G. Kasetty et al.

44

Fig. 4 OPN binds and neutralizes the cytotoxic effects of histones. **a** Surface plasmon resonance (SPR) sensorgrams illustrating interactions between different histone subunits (i.e., H1, H2A, H2B, H3.1, and H4) (ligand) and OPN (analyte). Histone subunits were covalently bound to a CM5 sensor chip using a standard amine-coupling kit. Different concentrations of OPN (62.5, 125, 250, 500, and 1000 nM) in running buffer were injected over the sensor chip to determine binding. The curves obtained after OPN injection were analyzed to show binding incidence with association and dissociation curves between H1, H2A, H2B, H3.1, H4, and OPN. **b** Possible interference of OPN with the histone-induced cytotoxic effects against human bronchial epithelial cells (BEAS-2B cells). The histones H1, H2A, H2B, H3.1, and H4 alone or a mixture of histones derived from calf thymus (CTH), or histones preincubated with OPN at a ratio of 1:1 were used. The cytotoxicity of histones is presented as percentage LDH release of the total LDH content. **c** Membrane permeability effects of histone subunits or CTH in the presence and absence of OPN against human endothelial cells (EA.hy926) are presented as fluorescence dye leakage. **d** Hemolytic activity of histone subunits or CTH in the presence and absence of OPN against human erythrocytes is presented as percentage hemolysis. OPN had a strong protective effect against both histone-induced cytotoxicity and hemolysis. The results are mean ± SEM ($n = 3$)

(Supplementary Table 3). Citrullination of histones has only been described in the tail regions, not in the globular domain.[43] Both native and citrullinated fragments bound OPN, but the latter to a lower degree (Fig. 5).

Phosphorylation of OPN affects the binding affinity with histones
Phosphorylation of OPN is essential for the function of the protein and contributes to its negative charge.[44] To elucidate the importance of OPN posttranslational modifications in binding to histones, SPR was performed. Three different forms of OPN were investigated in histone-binding experiments, i.e., recombinant OPN expressed in human HEK 293 cells (OPN), recombinant OPN expressed in *E. coli* (rec-OPN), and recombinant OPN expressed in HEK 293 cells treated with tartrate-resistant acid phosphatase (TRAP-OPN). The different forms of OPN were injected over sensor chips with immobilized histone subunits. Interestingly, both rec-OPN (lacking all posttranslational modifications) and TRAP-OPN (lacking negatively charged phosphate groups) showed reduced or no binding to the histone subunits (Fig. 6a). In contrast, OPN expressed in human (HEK 293) cells bound histones with high affinity, as indicated by the K_D values shown in Fig. 6b. However, the binding of OPN to histone H2B was weaker. To further demonstrate the importance of OPN phosphorylation with regard to its protective effects against histone-mediated cytotoxicity,

epithelial cells were incubated with histones in the presence or absence of OPN, rec-OPN, and TRAP-OPN at 1:1 ratios. OPN expressed in human (HEK 293) cells significantly reduced the LDH release from the cells protecting from histone-mediated toxic effects. Preincubation of histones with heparin was used as a positive control and efficiently neutralized the cytotoxic effects of histones (Fig. 6c).

OPN inhibits histone-induced formation of NETs
NETs have cytotoxic properties and they are a source of extracellular histones, thus providing a vicious inflammation-promoting circle.[9,11,15] We first investigated whether histones induced the formation of NETs in purified neutrophils. CTH were incubated with purified neutrophils, which was followed by staining of DNA scaffolds decorated with the granule-protein neutrophil elastase, serving as a marker for NETs. The histones did indeed cause morphological changes in neutrophils, leading to expulsion of their DNA into the extracellular space (Fig. 7a). Upon preincubation of histone with OPN at a ratio of 1:1, the NETs-inducing activity of histones was significantly reduced (Fig. 7b). In addition, to assess the level of NETs release from human neutrophils, levels of myeloperoxidase (MPO) (Fig. 7c) and extracellular DNA content (Fig. 7d) in the neutrophil cell supernatants were measured. Purified neutrophils were incubated with
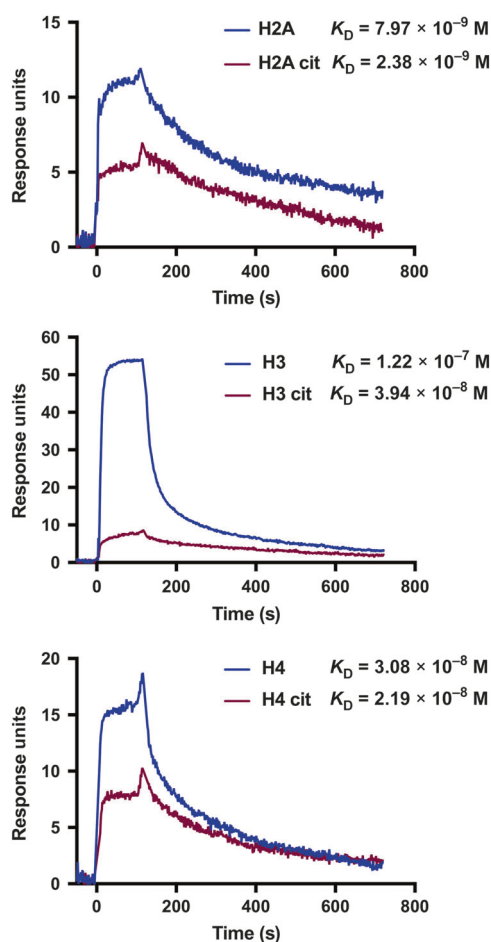
Osteopontin protects against lung injury caused by extracellular histones
G. Kasetty et al.

45

Fig. 5 OPN binds to citrullinated histone tails. SPR sensorgrams illustrating interactions between OPN and citrullinated histone tails. OPN was covalently bound to a CM5 sensor chip using a standard amine-coupling kit. Native and citrullinated peptides derived from H2A, H3, and H4 subunits were injected over the sensor chip to determine binding. Both native and citrullinated fragments bound OPN, but the latter to a lower degree

histones in the presence or absence of OPN, and the supernatants were collected. In accordance with previous results, OPN significantly inhibited the activation of neutrophils, thereby preventing the formation of NETs.

DISCUSSION

In this study, we found that OPN, an anionic protein that is highly expressed in the airways, binds and inhibits the pro-inflammatory and cytotoxic effects of extracellular histones. OPN is unstructured in solution and consists of 300 amino acids, almost one-third of which are negatively charged (i.e., aspartic acid or glutamic acid). In addition, the molecule is posttranslationally modified, including glycosylation with sialic acid residues and extensive phosphorylation.[20] Altogether, this makes OPN highly anionic and able to bind the cationic extracellular histones through electrostatic interaction, as shown in this study. In a previous study, OPN was found to bind to several cationic host defense molecules with high affinity, with the exception of LL-37 and lysozyme, suggesting some selectivity in binding cationic molecules.[45] It may also bind other DAMPs, preventing tissue injury. This could be investigated in future studies. The current study elucidates the importance of posttranslational modification of OPN, in

particular, phosphorylation is crucial for the cytoprotective role against cationic extracellular histones.

OPN can act as a chemoattractant for macrophages and neutrophils since it has integrin-binding motifs in its sequence.[46] However, there is a constitutive production of OPN in healthy airways, not causing any inflammation. In addition, OPN deficiency did not result in an altered recruitment of neutrophils during pneumococcal airway infection.[47] It may be that OPN in the healthy airway lumen is less important as an immunoregulatory molecule while in other contexts it plays additional active roles (e.g., executing cytokine-like activities and participating in tissue remodeling). It has been demonstrated that OPN prevents tissue injury in animal models of renal ischemia, cardiac, and hepatic reperfusion injury as well as ischemic stroke.[27–31] One possible explanation is that an RGD motif induces Akt and p42/p44 MAPK phosphorylation, resulting in tissue protection.[28] Bearing in mind the strong electrostatic interactions and substantial levels of OPN and histone–OPN complexes detected in the airways of ARDS patients and in individuals with acute lung injury, it seems more likely that OPN protects against the effects of extracellular histones through direct binding, superceding its actions as a cytokine, at least in the models used in this study. The levels of OPN increased during inflammation, suggesting an augmented capacity to attenuate cytotoxic effects of extracellular histones generated during the host response. However, one should bear in mind that the interaction between OPN and extracellular histones may eventually be saturated during severe inflammation, limiting the protection against tissue damage.

From where do the extracellular histones in the airways originate? In polymicrobial sepsis, histones appeared in plasma and also in a multiorgan pattern, including the lungs, where histones and neutrophils appeared together—with evidence of formation of NETs.[48] This was also the case in trauma patients, where circulating histones caused lung injury and triggered the formation of NETs.[36] However, in the models used in this study, extracellular histones are instilled or appear in the conducting airways. This is also the site of formation of NETs that are a significant source of extracellular histones, and NETs themselves contribute to tissue injury.[4,9,12,49,50] In the case of NETs, both histones and neutrophil granule proteins are responsible for the cytotoxicity.[15] Histones trigger pro-inflammatory responses through activation of TLR2, TLR4, and TLR9 on phagocytes.[51] Thus, histone-induced formation of NETs can be induced by TLR activation but cytolytic effects of extracellular histones on neutrophils may be of importance. Most likely, OPN binding to histones prevents receptor activation. NETs can also activate platelets to release TGF-β, leading to long-term consequences, such as tissue remodeling during the later phases of ALI/ARDS.[52] The cytotoxic activities of extracellular histones may also be neutralized by electrostatic binding to extracellular DNA, present at sites of inflammation, for example, in NETs. However, the deiminase PADI4 unwinds the DNA from histones of the nucleosomes during formation of NETs, resulting in exposure of free histones to the extracellular environment. Thus, despite presence of DNA, NETs mediate cytotoxic activity and histones play a major role in this context.[15] It is therefore possible that OPN plays protective roles also in the presence of extracellular DNA. Taken together, the inhibitory effect of OPN with regard to NET formation is likely to be important, reducing the tissue injury sustained and also remodeling during prolonged inflammation.

Several molecules have been described as being inhibitors of extracellular histone activity in ALI, many of them having anionic properties. Interestingly, C-reactive protein (CRP), an acute-phase reactant, protects against the toxicity of histones released into the circulation after extensive cell death.[53] Similar to OPN, CRP has anionic properties but these are less pronounced. C1 esterase inhibitor (C1INH) reduces bleomycin-induced lung injury through binding of extracellular histones. The binding of histones is not
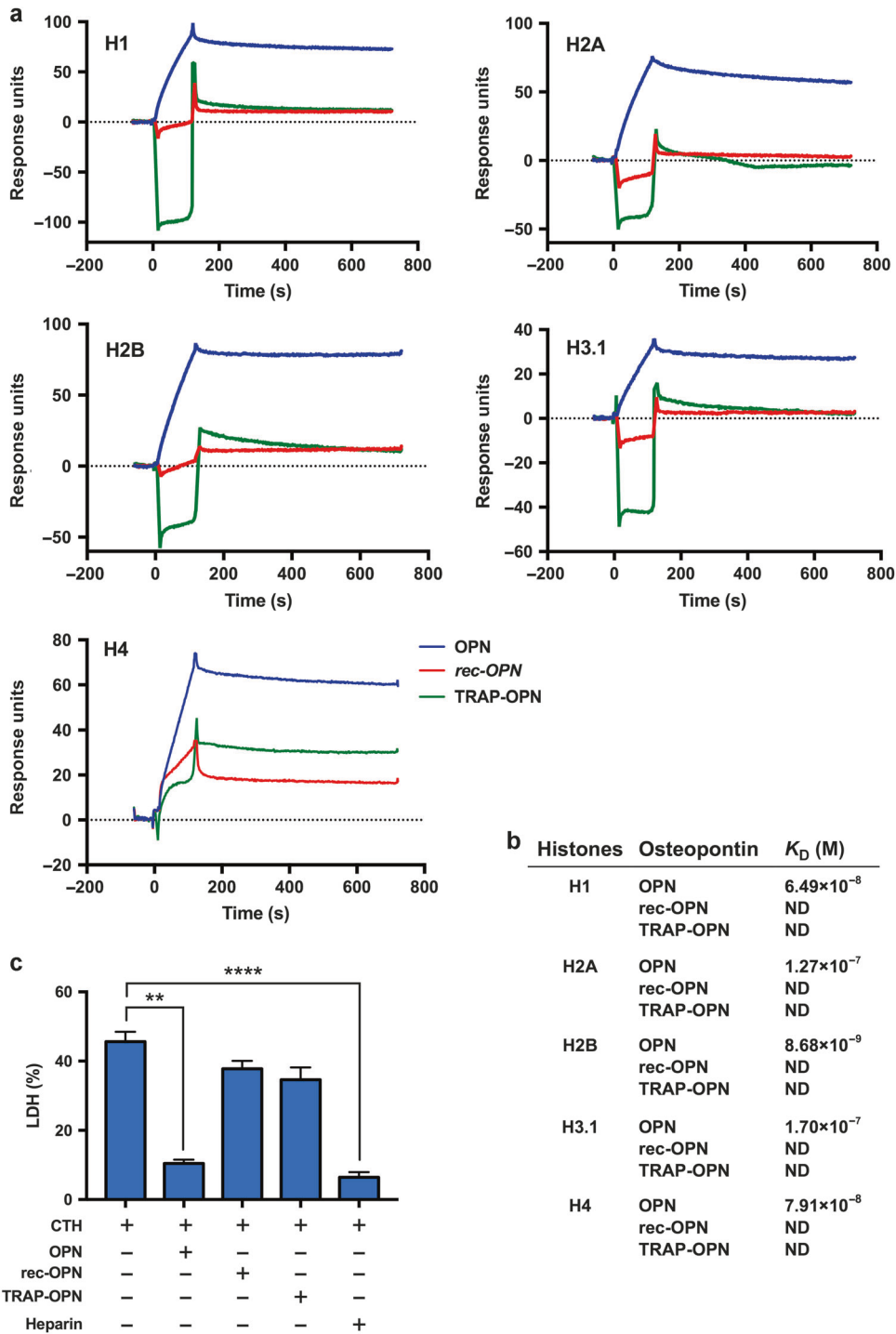
Osteopontin protects against lung injury caused by extracellular histones
G. Kasetty et al.

46

Fig. 6 Phosphorylation of OPN is essential for binding to histones and cytoprotective effects. **a** SPR sensorgrams showing differences in binding affinities between histone subunits (i.e., H1, H2A, H2B, H3.1, and H4) and different forms of OPN (expressed in HEK 293 cells (OPN), recombinant *E. coli* expressed OPN (rec-OPN), and tartrate-resistant acid phosphatase-treated OPN (TRAP-OPN) were compared. Histone subunits were covalently bound to a CM5 sensor chip using a standard amine-coupling kit. Different OPN at a concentration of 2 μM were injected over the sensor chip to determine binding. The binding affinity of OPN expressed in HEK 293 cells was higher compared to rec-OPN (lacking posttranslational modification) and TRAP-OPN (dephosphorylated using TRAP enzyme). **b** Table showing the K_D values obtained from SPR-binding studies. The K_D values for rec-OPN and TRAP-OPN were not determined because of low or no interaction and therefore denoted as not determined (ND). **c** LDH levels in the supernatants of human bronchiolar epithelial cells after incubation with calf thymus histones (CTH) in the presence and absence of OPN at a ratio of 1:1. The cytotoxicity of histones is presented as percentage LDH release of the total LDH content. The results are mean ± SEM ($n = 5$; **$P = 0.0050$, ****$P = < 0.0001$)

Osteopontin protects against lung injury caused by extracellular histones
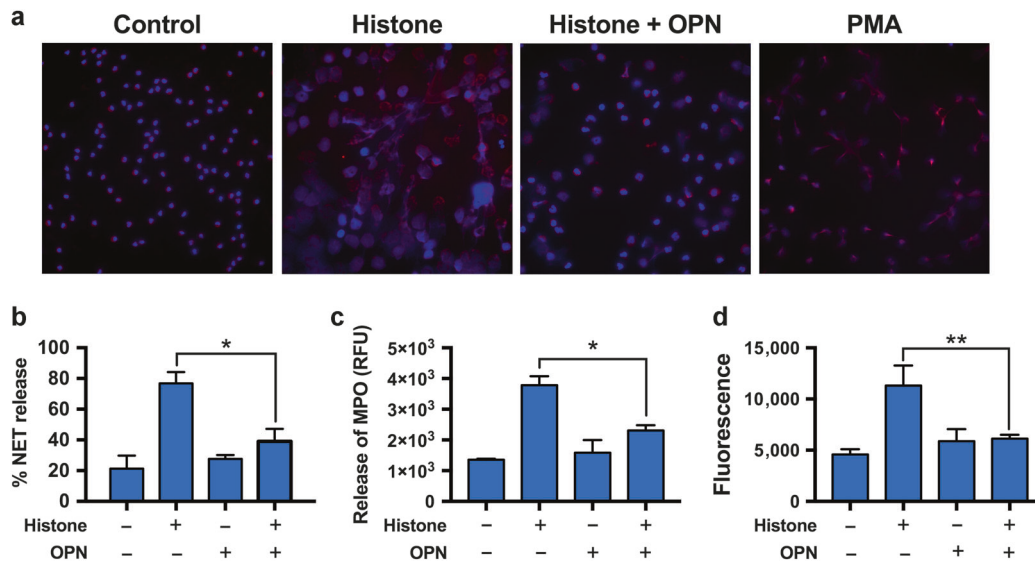G. Kasetty et al.

47

Fig. 7 OPN inhibits histone-induced NETs formation. **a** The release of NETs by neutrophils after exposure to histones in the presence or absence of OPN was assessed by fluorescence microscopy. Freshly isolated human neutrophils were preincubated with CTH (50 µg/mL) in the presence (1:1) or absence of OPN for 3 h at 37 °C. NETs release was detected by fluorescence microscopy using antibodies to neutrophil elastase (red) and staining of DNA by DAPI (blue) under ×40 magnification. PMA-stimulated neutrophils releasing NETs were used as a positive control. **b** The formation of NETs was quantified and is presented as the percentage of cells forming NETs. The effect of preincubation of CTH with OPN is also shown. $n = 6$; $*P = 0.0022$. **c** The effect of OPN on histone-induced MPO release from neutrophils was measured and is expressed as relative fluorescence units (RFU). **d** The release of NETs-associated DNA from activated neutrophils was quantified in the cell supernatant by PicoGreen analysis. Preincubation of OPN with CTH significantly reduced the amounts of DNA released into the supernatants ($n = 5$; $**P = 0.0079$)

dependent on its protease inhibitory activity, but is dependent on the glycosylation status.[37] Similar to OPN, other highly anionic molecules, e.g., glycosaminoglycans, protect against histone-induced tissue injury. This includes chondroitin sulfate and high-molecular-weight hyaluronan associated with inter-α inhibitor protein, as well as non-anticoagulant heparin in models of histone-induced systemic inflammation.[35,54] The protective effect against ALI mediated by these large, anionic molecules may be executed by mechanisms similar to those of OPN.

The reduction of pulmonary edema in the presence of OPN during lung injury seen in this study is important, since this is one of the major complications in ALI and ARDS, sometimes requiring extracorporeal membrane oxygenation.[1]

Overall, this study has shown for the first time that OPN has a crucial function as an anti-inflammatory and cytoprotective molecule, preventing the potentially harmful effects of extra-cellular histones in the airways during ALI. Thus, increased levels of OPN in the airways may play a protective role against cytotoxic effects exerted by cationic DAMPs.

METHODS
Animals
Male mice of the strain C57BL/6J (wild type; WT) and OPN$^{-/-}$ mice (8–10 weeks old) were bred and genotyped at Lund University. The OPN$^{-/-}$ mice have been described elsewhere.[55] The mice were housed under pathogen-free conditions and had free access to commercial chow and water.

Mouse models of acute lung injury
Direct instillation of histones in the airways is known to cause acute lung injury (ALI).[5] In the current study, mice were anesthetized, and 50 µg/g body weight of histones purified from calf thymus (CTH; Sigma-Aldrich, St Louis, MO) were instilled intranasally. The control mice received vehicle alone (PBS). For evaluation of animal survival, mice showing the defined and approved humane endpoint criteria (immobilization and shaking)

were euthanized with an overdose of isoflurane (Abbott Laboratories, North Chicago, IL) and counted as non-survivors.

In the case of LPS-induced ALI, mice were anesthetized, and 2 µg/g body weight of LPS (Escherichia coli, O111:B4; Sigma-Aldrich) was instilled intranasally. For evaluation of inflammatory indices in both models, mice were killed 16 and 8 h post challenge, respectively. For retrieval of bronchoalveolar lavage fluids (BALFs), the airways were flushed with 1 mL of PBS containing 0.1 mM EDTA. When needed, red blood cells were removed by resuspending the BALF cells in 100 µL of lysis buffer (150 mM NH_4Cl, 10 mM $KHCO_3$, and 0.1 mM EDTA; pH 7.2) for 2 min at room temperature (RT) followed by washing in 1 mL PBS. Cell-free BALF samples were stored at −80 °C until further analysis.

P. aeruginosa inoculation and determination of bacterial colony-forming units
P. aeruginosa (strain Xen 41) was grown to logarithmic phase (OD$_{620}$~0.5), harvested, washed in PBS and diluted in the same buffer to 2×10^8 cfu/mL. Each animal was infected with intranasal instillation of 50 µl bacteria. For the experiments measuring infection and inflammatory indices, mice were killed ~24 h post infection. BAL was performed and lungs were harvested to determine the bacterial colony-forming units (cfu). The lungs were mechanically homogenized and serial dilutions were subsequently plated on TH agar plates and incubated overnight at 37 °C in order to enumerate the cfu present.

Human ARDS BALF samples
BALF samples from 22 patients with moderate-to-severe ARDS (direct ARDS, $n = 13$ (pneumonia, $n = 11$; gastric aspiration, $n = 2$); indirect ARDS, $n = 9$ (sepsis, $n = 8$; trauma/surgery, $n = 1$)), according to the updated Berlin definition[2] were investigated. BALF was obtained by flexible fiberoptic bronchoscopy within 24 h following diagnosis. Fourteen healthy volunteers served as controls. Demographic and baseline clinical characteristic of the patient cohort and controls are described in the online data supplement.[37]

Human lung injury BALF samples

BALF samples from eight healthy individuals (six men and two women) were obtained before and 24 h after a 3 h of exposure in a swine confinement facility. Details of enrollment, the study protocol, and BALF sampling techniques have been published elsewhere.[38]

Wet-to-dry lung weight ratio

The left lobe was used to assess the lung wet-to-dry weight ratio by the gravimetric method. After the wet lung weight was measured, the lung was incubated at 60 °C for 48 h. Then, the dry lung weight was measured and ratio between wet and dry left lung weights was calculated.

Assessment of aspartate aminotransferase (AST)

Following instillation with CTH, the mice were killed after 16 h and blood was collected in EDTA tubes. Plasma was separated by centrifugation at $1500 \times g$ at 4 °C for 10 min and the samples were stored at −80 °C until analysis. The levels of AST in plasma were assessed using an assay reflecting AST enzymatic activity (Sigma-Aldrich) according to the manufacturer's instructions.

Measurement of parameters in BALF

To determine different parameters in BALF of mice and human samples, commercially available ELISAs were used to measure OPN (R&D Systems), lactate dehydrogenase (LDH) (USCN Life Science, Wuhan, China), and albumin (Bethyl Laboratories, Montgomery, TX), respectively. For detection of multiple mediators, the Bioplex Pro mouse cytokine assay, 23-Plex Group I was used on a Luminex-xMAP/Bioplex-200 System with Bioplex Manager 5.0 software (Bio-Rad, Richmond, CA).

Human lung tissue immunohistochemistry

Lung tissues were obtained from patients undergoing surgery for lung cancer or undergoing lung transplantation. Tissue samples were submerged in 4% buffered paraformaldehyde. After dehydration and paraffin embedding, 3 μm thin parallel sections were generated from the tissue blocks. After rehydration and antigen retrieval, sections were incubated with antibodies against histone H4 (rabbit polyclonal antibody, Abcam, Cambridge, UK) and OPN (a polyclonal rabbit antibody generously provided by the late Dr. Dick Heinegård, Lund). Bound antibodies were visualized using horseradish peroxidase-conjugated secondary antibodies. Histone H4 was visualized using 3,3-diaminobenzidine as chromogen (Dako, Glostrup, Denmark) and OPN was visualized using Vina green (Biocare Medical LLC, Concord, CA).

Surface plasmon resonance spectrometry

Binding characteristics between OPN and histone subunits were carried out using a BIAcore X100 instrument (GE Healthcare, Uppsala, Sweden). Human recombinant histone subunits (H1, H2A, H2B, H3.1, and H4; New England Biolabs, Ipswich, MA) were immobilized on a CM5 sensor chip. Interaction experiments were performed with injections of 62.5, 125, 250, 500, and 1000 nM of OPN in PBS. Dissociation was performed with PBS, followed by regeneration with Glycine-HCl (pH 1.5) for 60 s. The BIA evaluation 3.1 analysis software (GE Healthcare) was used to determine equilibrium dissociation constants (K_D) from the processed data sets by fitting to a 1:1 molecular binding model with drifting baseline.

In a separate experiment affinities of histone subunits to different forms of OPN, expressed in HEK 293 cells (OPN), recombinant *E. coli* expressed OPN (rec-OPN), and OPN treated with tartrate-resistant acid phosphatase (R&D systems) (TRAP-OPN) were compared. The CM5 sensor chips coated with histone subunits were used for the binding assay. Different OPN proteins were injected at a concentration of 2 μM at a flow rate of 10 μl/min followed by dissociation and regeneration steps as described above.

In experiments illustrating interactions between OPN and citrullinated histone tails. OPN was covalently bound to a CM5 sensor chip. Native and citrullinated peptides derived from H2A, H3, and H4 subunits at a concentration of 1 μM were injected over the sensor chip to determine binding.

Dephosphorylation of osteopontin

The dephosphorylation of OPN was performed as described elsewhere.[56] In brief, OPN (50 μg) was incubated in the presence or absence of 5 milliunits of recombinant tartrate-resistant acid phosphatase (TRAP) (R&D systems, Abingdon, UK), in 10 mM acetate buffer, pH 5.8, 50 μM EDTA for 4 h at 37 °C. After incubation, pH of the solution was adjusted to 7.4 by adding NaOH.

In vitro hemolysis assay

Human EDTA blood (1 mL) was centrifuged, the plasma was removed and after washings replaced by 1 mL of PBS. After titration experiments, histone subunits were diluted in PBS to a final concentration of 10 μM while CTH were used at a final concentration of 100 μg/mL in the presence or absence of OPN at a ratio of 1:1. Triton X-100 (2% v/v in PBS) and PBS served as a positive and negative controls, respectively. Ten microliters of washed erythrocytes (5% v/v) were added to each sample followed by incubation during rotation for 60 min at 37 °C. All samples were centrifuged and the supernatants were transferred to microtiter plates. The absorbance of hemoglobin was measured at 540 nm and histone-induced hemolysis was expressed as a percentage of Triton X-100-induced hemolysis.

Histone-induced cytotoxicity

To investigate histone-induced toxicity on airway epithelial cells, a human bronchial epithelial cell line (BEAS-2B cells; ATCC, Rockville, MD) was used. The cells were cultured in RPMI with GlutaMAX containing 10% fetal bovine serum, and 100 U/mL penicillin/streptomycin. The adherent cells were grown confluent in microtiter plates and washed in 200 μL of RPMI prior to the experiments. After titration experiments, histone subunits (4 μM) or CTH (100 μg/mL) were diluted in phenol-free RPMI and preincubated with OPN at a ratio of 1:1 for 1 h at 37 °C. Samples were transferred to the epithelial cells and incubated overnight (16 h at 37 °C and 5% CO_2). Supernatants were then transferred onto new microtiter plates and one volume of a LDH substrate mix was added. LDH release was measured at 490 nm using the Tox-7 kit (Sigma-Aldrich) according to the manufacturer's instructions. Histone-induced LDH release was calculated as percent of the release obtained using Triton X-100 (1%) to lyse the cells.

Permeability assay

The in vitro permeability of a confluent monolayer of endothelial cells was analyzed in a dual chamber system using FITC-Dextran according to the manufacture's instructions (Millipore, USA). In brief, 200 μL (1×10^6) EA.hy926 cells were seeded on the upper chamber of transwell polycarbonate membranes (24-well, polycarbonate filters, 0.4 μm pore size, Corning) and the lower chambers filled with 500 μL of DMEM (supplemented with 10% FBS and anti–anti). Cells were then grown for 3 days at 37 °C to obtain a monolayer and treated with histones in DMEM supplemented with 2% FBS for 1 h. Permeability was then assessed by replacing the media in the upper chamber with 150 μL FITC-Dextran (1:40 dilution) and in the lower chamber with 500 μL DMEM media. After 20 min, a 100 μL aliquot was taken from the lower chamber into a 96-well opaque plate and the fluorescence was measured at 485 nm and 535 nm excitation and emission, respectively.

Osteopontin protects against lung injury caused by extracellular histones
G. Kasetty et al.

49

Histone-induced NETs and immunofluorescence microscopy
Neutrophils were isolated from whole blood using Lymphoprep (Axis-Shield, Norway) and were seeded onto poly-L-lysine-coated coverslips. NETs were induced by stimulating neutrophils with histones (CTH) at a concentration of 50 µg/mL in the presence or absence of OPN at a ratio of 1:1 for 3 h at 37 °C and in the presence of 5% CO_2. Neutrophils incubated with PMA (20 nM) in RPMI 1640 were used as positive controls. Cells were fixed, permeabilized, and probed with antibodies against neutrophil elastase. Secondary antibodies conjugated with Alexa594 (Lifetech, Carlsbad, CA) were added and samples were mounted in ProLong Gold anti-fade reagent with DAPI (Lifetech). Samples were investigated using a Nikon microscope with a ×20 objective. NETs were analyzed and quantified using a method described previously.[57] Image analysis was performed with a public-domain software (Fiji). For quantification of NETs or DNA, a spectro-fluorometric method was conducted using the Quant-iT™ Pico-Green® dsDNA kit (Invitrogen, Carlsbad, CA) as previously described.[58]

SDS-PAGE and western blot
BALF samples from mice with LPS-induced ALI and controls were separated using SDS-PAGE (8–16% Mini-PROTEAN TGX gels; Bio-Rad Laboratories, Hercules, CA) under reducing conditions. Proteins were transferred to a PVDF membrane (0.45 µm, Immobilon-P; Merck-Millipore), blocked by 3% (w/v) skimmed milk, washed, and incubated with rabbit polyclonal anti-Histone H3 antibody. The washed membrane was incubated with HRP-conjugated secondary antibodies (1:2000; Dako, Glostrup, Denmark) and immobilized antibodies were visualized by peroxide solution and the luminol/enhancer solution (1:1 v/v) (SuperSignal West Pico Chemiluminescent Substrate; Thermo Fischer Scientific).

Detection of histone–OPN complexes in BALF
A microtiter plate was coated with 10 µg/mL anti-histone antibody (Roche Diagnostica) in 50 mM $NaHCO_3$, pH 9.6, at 4 °C overnight. After washing with PBS containing 0.1% Tween 20 (PBST), the plate was blocked with 1% BSA in PBS at room temperature for 1 h. BALF (50 µL) was added into wells and then the plate was incubated at 37 °C for 1 h. Next, the plate was extensively washed with PBST and incubated with an anti-OPN antibody (R&D Systems) at room temperature for 2 h. After washing with PBST, a peroxidase-conjugated antibody was added and color reaction was developed using a peroxidase-specific substrate, TMB (Thermo Fisher Scientific) according to the manufacturer's instruction. To discriminate between specific vs non-specific interactions, control experiments without BALF or with IgG isotype control were performed.

Scanning electron microscopy
For scanning electron microscopy (SEM), lungs were collected at 8 or 16 h after intranasal instillation of histones or LPS, respectively. The tissue samples were fixed in 2.5% (v/v) glutaraldehyde in 0.15 M sodium cacodylate buffer, pH 7.4, overnight at room temperature. Specimens were washed with cacodylate buffer, and dehydrated with increasing amounts of ethanol. Next, the specimens were subjected to critical-point drying in carbon dioxide, mounted on aluminum holders, sputtered with 30 nm palladium/gold, and analyzed using a Phenom ProX desktop scanning electron microscope (Phenom-World, Eindhoven, the Netherlands) with an acceleration voltage of 10 kV.

Statistical analysis
Data were expressed as the mean ± standard error of the mean (SEM) and were analyzed using Student's t test. For statistical evaluation of more than two experimental groups, one-way analysis of variance (ANOVA) with Dunn's multiple comparisons post-test was used. All statistical evaluations were performed using GraphPad Prism software 6.0 (GraphPad Software, La Jolla, CA). Any P values greater than 0.05 were considered non-significant. Asterisks in the tables and figures are used to represent different levels of significance as follows: *$P \le 0.05$, **$P \le 0.01$, ***$P \le 0.001$, and ****$P \le 0.0001$.

AUTHOR CONTRIBUTIONS
Conception and design of the study: G.K. and A.E. Acquisition, analysis, and interpretation of data: G.K., R.K.V.B., P.P., M.N.A., M.M., M.W., J.S.E., L.P., H.H. and A.E. Drafting of the article or revising it critically for important intellectual content: G.K., H.H. and A.E.

ADDITIONAL INFORMATION
The online version of this article (https://doi.org/10.1038/s41385-018-0079-3) contains supplementary material, which is available to authorized users.

Conflict of interest: The authors declare no competing interest.

Ethics statement: All the human participants or their next-of-kin gave their written informed consent to participate in the study which was approved by the ethics committee of the Faculty of Medicine, Justus-Liebig-University, Giessen, Germany (No. 84/93 and No. 29/01), the Regional Ethical Review Board in Lund (entry no. LU412-03), and Karolinska Institutet, Solna (95–347). All mouse experiments were conducted according to the institutional guidelines and were approved by the Malmö-Lund Animal Care Ethics Committee (M138-13 and M187-15).

REFERENCES
1. Matthay, M. A. & Zemans, R. L. The acute respiratory distress syndrome: pathogenesis and treatment. *Annu. Rev. Pathol.* **6**, 147–163 (2011).
2. Force, A. D. T. et al. Acute respiratory distress syndrome: the Berlin definition. *JAMA* **307**, 2526–2533 (2012).
3. Gattinoni, L. et al. Acute respiratory distress syndrome caused by pulmonary and extrapulmonary disease. Different syndromes? *Am. J. Respir. Crit. Care Med.* **158**, 3–11 (1998).
4. Ward, P. A. & Grailer, J. J. Acute lung injury and the role of histones. *Transl. Respir. Med.* **2**, 1 (2014).
5. Bosmann, M. et al. Extracellular histones are essential effectors of C5aR- and C5L2-mediated tissue damage and inflammation in acute lung injury. *FASEB J.* **27**, 5010–5021 (2013).
6. Fattahi, F. et al. Selective biological responses of phagocytes and lungs to purified histones. *J. Innate Immun.* **9**, 300–317 (2017).
7. Rittirsch, D. et al. Acute lung injury induced by lipopolysaccharide is independent of complement activation. *J. Immunol.* **180**, 7664–7672 (2008).
8. Matute-Bello, G., Frevert, C. W. & Martin, T. R. Animal models of acute lung injury. *Am. J. Physiol. Lung Cell. Mol. Physiol.* **295**, L379–L399 (2008).
9. Liu, S. et al. Neutrophil extracellular traps are indirectly triggered by lipopolysaccharide and contribute to acute lung injury. *Sci. Rep.* **6**, 37252 (2016).
10. Lee, W. L. & Downey, G. P. Neutrophil activation and acute lung injury. *Curr. Opin. Crit. Care* **7**, 1–7 (2001).
11. Narasaraju, T. et al. Excessive neutrophils and neutrophil extracellular traps contribute to acute lung injury of influenza pneumonitis. *Am. J. Pathol.* **179**, 199–210 (2011).
12. Wu, D. et al. Apoptotic release of histones from nucleosomes. *J. Biol. Chem.* **277**, 12001–12008 (2002).
13. Kumar, S. V. et al. Neutrophil extracellular trap-related extracellular histones cause vascular necrosis in severe GN. *J. Am. Soc. Nephrol.* **26**, 2399–2413 (2015).
14. Kleine, T. J., Lewis, P. N. & Lewis, S. A. Histone-induced damage of a mammalian epithelium: the role of protein and membrane structure. *Am. J. Physiol.* **273**(6 Pt 1), C1925–C1936 (1997).
15. Saffarzadeh, M. et al. Neutrophil extracellular traps directly induce epithelial and endothelial cell death: a predominant role of histones. *PLoS ONE* **7**, e32366 (2012).

Osteopontin protects against lung injury caused by extracellular histones
G. Kasetty et al.

50

16. Xu, J. et al. Extracellular histones are major mediators of death in sepsis. Nat. Med. **15**, 1318–1321 (2009).

17. Allam, R. et al. Histones from dying renal cells aggravate kidney injury via TLR2 and TLR4. J. Am. Soc. Nephrol. **23**, 1375–1388 (2012).

18. Semeraro, F. et al. Extracellular histones promote thrombin generation through platelet-dependent mechanisms: involvement of platelet TLR2 and TLR4. Blood **118**, 1952–1961 (2011).

19. Huang, H. et al. Endogenous histones function as alarmins in sterile inflammatory liver injury through Toll-like receptor 9 in mice. Hepatology **54**, 999–1008 (2011).

20. Kazanecki, C. C., Uzwiak, D. J. & Denhardt, D. T. Control of osteopontin signaling and function by post-translational phosphorylation and protein folding. J. Cell. Biochem. **102**, 912–924 (2007).

21. Woodruff, P. G. et al. A distinctive alveolar macrophage activation state induced by cigarette smoking. Am. J. Respir. Crit. Care Med. **172**, 1383–1392 (2005).

22. Papaporfyriou, A. et al. Increased levels of osteopontin in sputum supernatant in patients with COPD. Chest **146**, 951–958 (2014).

23. Jovic, S. et al. Osteopontin is increased in cystic fibrosis and can skew the functional balance between ELR-positive and ELR-negative CXC-chemokines. J. Cyst. Fibros. **14**, 453–463 (2015).

24. Samitas, K. et al. Osteopontin expression and relation to disease severity in human asthma. Eur. Respir. J. **37**, 331–341 (2011).

25. Konno, S., Kurokawa, M., Uede, T., Nishimura, M. & Huang, S. K. Role of osteopontin, a multifunctional protein, in allergy and asthma. Clin. Exp. Allergy **41**, 1360–1366 (2011).

26. Hirano, Y., Aziz, M., Yang, W. L., Ochani, M. & Wang, P. Neutralization of osteopontin ameliorates acute lung injury induced by intestinal ischemia-reperfusion. Shock **46**, 431–438 (2016).

27. Persy, V. P., Verstrepen, W. A., Ysebaert, D. K., De Greef, K. E. & De Broe, M. E. Differences in osteopontin up-regulation between proximal and distal tubules after renal ischemia/reperfusion. Kidney Int. **56**, 601–611 (1999).

28. Meller, R. et al. Neuroprotection by osteopontin in stroke. J. Cereb. Blood Flow. Metab. **25**, 217–225 (2005).

29. Wang, Y., Chen, B., Shen, D. & Xue, S. Osteopontin protects against cardiac ischemia-reperfusion injury through late preconditioning. Heart Vessels **24**, 116–123 (2009).

30. Zhang, Z. X. et al. Osteopontin expressed in tubular epithelial cells regulates NK cell-mediated kidney ischemia reperfusion injury. J. Immunol. **185**, 967–973 (2010).

31. Patouraux, S. et al. Osteopontin deficiency aggravates hepatic injury induced by ischemia-reperfusion in mice. Cell Death Dis. **5**, e1208 (2014).

32. Gela, A. et al. Osteopontin binds and modulates functions of eosinophil-recruiting chemokines. Allergy **71**, 58–67 (2016).

33. Westman, J. et al. Extracellular histones induce chemokine production in whole blood ex vivo and leukocyte recruitment in vivo. PLoS Pathog. **11**, e1005319 (2015).

34. Westman, J. et al. Treatment with p33 curtails morbidity and mortality in a histone-induced murine shock model. J. Innate Immun. **6**, 819–830 (2014).

35. Wildhagen, K. C. et al. Nonanticoagulant heparin prevents histone-mediated cytotoxicity in vitro and improves survival in sepsis. Blood **123**, 1098–1101 (2014).

36. Abrams, S. T. et al. Circulating histones are mediators of trauma-associated lung injury. Am. J. Respir. Crit. Care Med. **187**, 160–169 (2013).

37. Wygrecka, M. et al. Antihistone properties of C1 esterase inhibitor protect against lung injury. Am. J. Respir. Crit. Care Med. **196**, 186–199 (2017).

38. Ek, A., Palmberg, L. & Larsson, K. Influence of fluticasone and salmeterol on airway effects of inhaled organic dust;an in vivo and ex vivo study. Clin. Exp. Immunol. **121**, 11–16 (2000).

39. Drent, M., Cobben, N. A., Henderson, R. F., Wouters, E. F. & van Dieijen-Visser, M. Usefulness of lactate dehydrogenase and its isoenzymes as indicators of lung damage or inflammation. Eur. Respir. J. **9**, 1736–1742 (1996).

40. Dicker, A. J. et al. Neutrophil extracellular traps are associated with disease severity and microbiota diversity in patients with chronic obstructive pulmonary disease. J. Allergy Clin. Immunol. **141**, 117–127 (2018).

41. Marcos, V. et al. CXCR2 mediates NADPH oxidase-independent neutrophil extracellular trap formation in cystic fibrosis airway inflammation. Nat. Med. **16**, 1018–1023 (2010).

42. Barrero, C. A. et al. Histone 3.3 participates in a self-sustaining cascade of apoptosis that contributes to the progression of chronic obstructive pulmonary disease. Am. J. Respir. Crit. Care Med. **188**, 673–683 (2013).

43. Rodriguez-Paredes, M. & Esteller, M. Cancer epigenetics reaches mainstream oncology. Nat. Med. **17**, 330–339 (2011).

44. Sorensen, E. S., Hojrup, P. & Petersen, T. E. Posttranslational modifications of bovine osteopontin: identification of twenty-eight phosphorylation and three O-glycosylation sites. Protein Sci. **4**, 2040–2049 (1995).

45. Gela, A. et al. Osteopontin that is elevated in the airways during COPD impairs the antibacterial activity of common innate antibiotics. PLoS ONE **11**, e0146192 (2016).

46. Morimoto, J., Kon, S., Matsui, Y. & Uede, T. Osteopontin; as a target molecule for the treatment of inflammatory diseases. Curr. Drug. Targets **11**, 494–505 (2010).

47. van der Windt, G. J. et al. Osteopontin impairs host defense during pneumococcal pneumonia. J. Infect. Dis. **203**, 1850–1858 (2011).

48. Fattahi, F. et al. Organ distribution of histones after intravenous infusion of FITC histones or after sepsis. Immunol. Res. **61**, 177–186 (2015).

49. Garcia, C. C. et al. Complement C5 activation during influenza A infection in mice contributes to neutrophil recruitment and lung injury. PLoS ONE **8**, e64443 (2013).

50. Villanueva, E. et al. Netting neutrophils induce endothelial damage, infiltrate tissues, and expose immunostimulatory molecules in systemic lupus erythematosus. J. Immunol. **187**, 538–552 (2011).

51. Silk, E., Zhao, H., Weng, H. & Ma, D. The role of extracellular histone in organ injury. Cell Death Dis. **8**, e2812 (2017).

52. Bosmann, M. & Ward, P. A. Protein-based therapies for acute lung injury: targeting neutrophil extracellular traps. Expert. Opin. Ther. Targets **18**, 703–714 (2014).

53. Abrams, S. T. et al. Human CRP defends against the toxicity of circulating histones. J. Immunol. **191**, 2495–2502 (2013).

54. Chaaban, H. et al. Inter-alpha inhibitor protein and its associated glycosaminoglycans protect against histone-induced injury. Blood **125**, 2286–2296 (2015).

55. Blom, T., Franzen, A., Heinegard, D. & Holmdahl, R. Comment on "The influence of the proinflammatory cytokine, osteopontin, on autoimmune demyelinating disease". Science **299**, 1845 (2003).

56. Ek-Rylander, B., Flores, M., Wendel, M., Heinegard, D. & Andersson, G. Dephosphorylation of osteopontin and bone sialoprotein by osteoclastic tartrate-resistant acid phosphatase. Modulation of osteoclast adhesion in vitro. J. Biol. Chem. **269**, 14853–14856 (1994).

57. Mohanty, T. et al. A novel mechanism for NETosis provides antimicrobial defense at the oral mucosa. Blood **126**, 2128–2137 (2015).

58. Berends, E. T. et al. Nuclease expression by Staphylococcus aureus facilitates escape from neutrophil extracellular traps. J. Innate Immun. **2**, 576–586 (2010).